

Neuron, Volume 65

Supplemental Information

Modulation of Visual Responses by Behavioral State in Mouse Visual Cortex

Cristopher M. Niell and Michael P. Stryker

Animal procedures

Experiments were performed on adult (age 2-4 month) female C57/Bl6 mice. The animals were maintained in the animal facility at University of California, San Francisco (UCSF) and used in accordance with protocols approved by the UCSF Institutional Animal Care and Use Committee. Animals were maintained on a 14hr light / 10hr dark cycle. Experiments were performed during the light phase of the cycle, because we found that during the dark phase, the animals often ran continuously, preventing a comparison of spontaneous alternation between stationary and moving.

Our spherical treadmill was based on the design of (Dombeck et al., 2007). Briefly, eight air inlets were attached to the bowl of an 8" (203 mm) steel ladle (McMaster-Carr). A closed-cell foam ball (Plasteel Corporation) placed inside the bowl provided a freely rotating surface on which the mouse stood. The animal's head was fixed via a surgically attached steel headplate that could be screwed into a rigid crossbar above the floating ball. The movement of the ball was measured with two optical mice via custom driver software, which transmitted the USB signals to our data analysis system.

Several days before recording, the custom stainless steel headplate was cemented to the skull to allow head fixation. Animals were anesthetized with isoflurane in oxygen (3% induction, 1.5-2% maintenance) and given a subcutaneous injection of carprofen (5mg/kg) as a post-operative analgesic, and 0.2ml of saline to prevent post-operative dehydration. Following a scalp incision, the fascia was cleared from the surface of the skull, and a thin layer of cyanoacrylate (VetBond, WPI Inc.) was applied, to provide a substrate to which the dental acrylic could adhere. The metal headplate was then attached with dental acrylic, covering the entire skull except for the region in the center opening of

the headplate, which was filled with a silicone elastomer (Kwik-Sil, WPI Inc.) to protect the skull. The animal was then allowed to recover.

On the days following headplate attachment, the animal was allowed to habituate to the recording setup, first by a period of handling by the experimenter, and then being allowed to stand on the surface of the ball. Finally, air pressure was applied to the ball and the headplate was screwed into the crossbar above the ball, and the animal was allowed to run freely. Although the animals initially had some difficulty balancing on the ball, they quickly (10-15 minutes) learned to stand still, walk, and run on the ball, even exhibiting grooming behavior (Supplemental Movie 1). Two 10-minute sessions of practice on the ball was generally sufficient for them to appear comfortable in the head-fixed arrangement.

On the day of recording, the animal was again anesthetized as described above. The silicone plug was removed, and a craniotomy ~1mm in diameter was made over visual cortex or the thalamus. The brain surface was covered with 2.5% agarose in saline, the headplate opening was again filled with silicone elastomer, and the animal was allowed to recover for 2-3 hours before recording.

For recording, the animal was placed in the head-holder on the floating ball, the silicone plug was removed, and a multisite electrode (Neuronexus Technologies) was inserted through the craniotomy and overlying agarose using a stereotax-mounted microdrive (Physik-Instrumente, Germany). For cortical recordings, we used a tetrode configuration, with four tetrode clusters, each consisting of four sites separated by 25 μ m on a side (model a2x2-tet-3mm-150-121). The electrode was placed at an angle of ~45deg relative to the cortical surface, to increase the distance between the insertion and recording sites, and inserted to a depth of <400 μ m below the cortical surface to record cells in layer 2/3. For recordings in dLGN, a linear probe configuration was used, with 16 sites separated by 50 μ m along a single shank (model a1x16-5mm50-177). The electrodes were inserted vertically at 2.2 mm lateral and 2.8 mm posterior from the bregma suture. At a depth of ~2500–3000 μ m, the dLGN could be identified by rapid firing in response to either ON or OFF flashes of a small spot at a specific location in the visual field. For both LGN and cortical recordings, the electrode was allowed to settle in one position for 30-45 minutes

to obtain stable single-unit recordings. The electrode was placed without regard for the presence of visually responsive units on individual sites, and all units stably isolated over the recording period were included in analysis. Following placement, the electrode was further embedded in agarose to increase mechanical stability.

A primary concern in implementing awake recordings in a running mouse was stability of the electrode relative to the brain tissue, to prevent both damage to cells and drift of recorded units. Indeed, the low reaction-force substrate provided by the floating ball, combined with the rigidity of the headplate fixation and support, results in minimal brain movements. In vivo two-photon imaging under similar conditions demonstrates movements of less than a few microns, allowing stable imaging of neurons and even dendritic spines over extended periods even during locomotion ((Dombeck et al., 2007) and our unpublished observations). Extracellular recordings are likely even more stable, as the electrode is coupled to brain movement, both by being inserted into the tissue and via mechanical linkage provided by agarose on the brain surface. Evidence of this stability is provided by our ability to record well-isolated, visually responsive units over extended periods.

During recording, the animal was allowed to behave freely, alternating between stationary and running behavior. Periods of grooming were demarcated by the experimenter, using a push-button interfaced with the data acquisition system. For each recording site, presentation continued until sufficient trials were performed to ensure that each stimulus condition was presented 5-7 times in each behavioral state. In several cases where the animal was still behaving well after one recording session, the electrode was either shifted in depth or re-inserted at a non-overlapping position, to sample a new set of units. In no cases was the electrode inserted more than twice, to avoid damage to cortex. Recordings continued for up to several hours, after which the animal was euthanized by overdose of barbiturates.

Visual stimuli, data acquisition, and analysis

Visual stimuli were presented as described previously (Niell and Stryker, 2008). Briefly, stimuli were generated in Matlab using the Psychophysics Toolbox extensions (Brainard,

1997; Pelli, 1997) and displayed with gamma correction on a monitor (Nanao Flexscan, 30 x 40 cm, 60 Hz refresh rate, 32 cd/m² mean luminance) placed 25 cm from the mouse, subtending ~60-75° of visual space. For LFP measurements, we presented full-length drifting bars (width 5°, velocity 30°/sec, 16 directions), as these evoked robust power in the gamma range. To characterize neural responses with single unit recordings, we presented drifting sinusoidal gratings of 1.5 s duration at 100% contrast, with temporal frequency of 2 Hz, spatial frequency of 0.01, 0.02, 0.04, 0.08, 0.16, 0.32, and 0 cycles/° (cpd), i.e., full-field flicker. For cortex, we presented 12 evenly spaced directions, while in the LGN we only presented 4 directions, since most LGN units were not orientation selective. The stimulus conditions were randomly interleaved, and a gray blank condition (mean luminance) was included to estimate the spontaneous firing rate.

Movement signals from the optical mice were acquired in an event-driven mode at up to 300Hz, and integrated at 100msec intervals. We then used these measurements to calculate the net physical displacement of the top surface of the ball. We determined the average speed during a stimulus presentation to classify the trial as stationary (<1cm/sec) or moving (>1 cm/sec).

Data acquisition was performed as described by Niell and Stryker (Niell and Stryker, 2008). Signals were acquired using a System 3 workstation (Tucker-Davis Technologies) and analyzed with custom software in Matlab (MathWorks). For local field potential (LFP) analysis, the extracellular signal was filtered from 1 to 300 Hz and sampled at 1.5 kHz. The power spectrum was computed using multi-taper estimation in Matlab with the Chronux package (<http://chronux.org/>), (Mitra and Bokil, 2008), using a three second sliding window and 3-5 tapers. Spectra were normalized for presentation by applying a 1/f correction (Sirota et al., 2008).

For single-unit activity, the extracellular signal was filtered from 0.7 to 7 kHz and sampled at 25 kHz. Spiking events were detected on-line by voltage threshold crossing, and a 1 ms waveform sample on all 4 recording surfaces of the tetrode was acquired around the time of threshold crossing. Single-unit clustering and spike waveform analysis was performed as described previously (Niell and Stryker, 2008), with a combination of custom software in Matlab and Klusta-Kwik (Harris et al., 2000). Quality of separation

was determined based on the Mahalanobis distance and L-ratio (Schmitzer-Torbert et al., 2005) and evidence of a clear refractory period. Nearly all units were stable in terms of amplitude and waveform over the course of an hour recording time; units were also checked to assure that they responded similarly at the beginning and end of recording to ensure that they had not drifted or suffered mechanical damage. Typical recordings yielded 6-12 single units across the electrode, with 1-4 per tetrode group. In both the LGN and layer 2/3 of cortex, most units appeared predominantly on a single recording site, although units often contributed a signal below the voltage threshold on neighboring sites, which allowed improved unit discrimination.

As previously (Niell and Stryker, 2008), units were classified as narrow or broad spiking based on properties of their average waveforms, at the electrode site with largest amplitude. Three parameters were used for discrimination: the height of the positive peak relative to the initial negative trough, the time from the minimum of the initial trough to maximum of the following peak, and the slope of the waveform 0.5 ms after the initial trough.

The average spontaneous rate for each unit was calculated by averaging the rate over all blank condition presentations. For cortical recordings, responses at each orientation and spatial frequency were calculated by averaging the spike rate during the 1.5 s presentation and subtracting the spontaneous rate. The preferred orientation was determined by averaging the response across all spatial frequencies, and calculating half the complex

phase of the value $\frac{\sum F(\theta)e^{2i\theta}}{\sum F(\theta)}$. The orientation tuning curve was constructed for the

spatial frequency that gave peak response at this orientation. Given this fixed preferred orientation θ_{pref} , the tuning curve was fitted as the sum of two Gaussians centered on θ_{pref} and $\theta_{\text{pref}}+\pi$, of different amplitudes A_1 and A_2 but equal width σ , with a constant baseline B . From this fit, we calculated two metrics – an orientation selectivity index (OSI) representing the ratio of the tuned versus untuned component of the response, and the width of the tuned component. OSI was calculated as the depth of modulation from the preferred orientation to its orthogonal orientation $\theta_{\text{ortho}} = \theta_{\text{pref}}+\pi/2$, as $(R_{\text{pref}} - R_{\text{ortho}})/(R_{\text{pref}} + R_{\text{ortho}})$.

+ R_{ortho}). Tuning width was the half-width at half-maximum of the fit above the baseline, R_{ortho} .

For LGN recordings, spike responses for each condition were binned in 100ms intervals, with the average spontaneous rate subtracted. The F1 and F0 components of the response were then calculated by fast Fourier transform. Response amplitude was averaged over the four directions presented, at the spatial frequency that gave the largest response.

Bursts were defined following (Grubb and Thompson, 2005), as a group of spikes with interspike interval <4msec following a period without spikes of at least 100msec, which has been shown to demarcate the vast majority of events associated with de-inactivation of T-type calcium channels (Lu et al., 1992).

Eye movements were recorded with a Canon S3-IS 12X-zoom digital camera with macro lenses. Video files were imported into Matlab, and pupil position was marked manually at 250msec intervals. Translational movement of the pupil was converted to angular rotation of the eye based on the published anatomical value for the rotational radius of the pupil, 1.14mm (Remtulla and Hallett, 1985).

Statistical significance was calculated by Mann-Whitney U test. For figures presenting median values, error bars represent the standard error of the median as calculated by a bootstrap.

Brainard, D. H. (1997). The Psychophysics Toolbox. *Spat Vis* 10, 433-436.

Dombeck, D. A., Khabbaz, A. N., Collman, F., Adelman, T. L., and Tank, D. W. (2007). Imaging large-scale neural activity with cellular resolution in awake, mobile mice. *Neuron* 56, 43-57.

Grubb, M. S., and Thompson, I. D. (2005). Visual response properties of burst and tonic firing in the mouse dorsal lateral geniculate nucleus. *J Neurophysiol* 93, 3224-3247.

Harris, K. D., Henze, D. A., Csicsvari, J., Hirase, H., and Buzsaki, G. (2000). Accuracy of tetrode spike separation as determined by simultaneous intracellular and extracellular measurements. *J Neurophysiol* 84, 401-414.

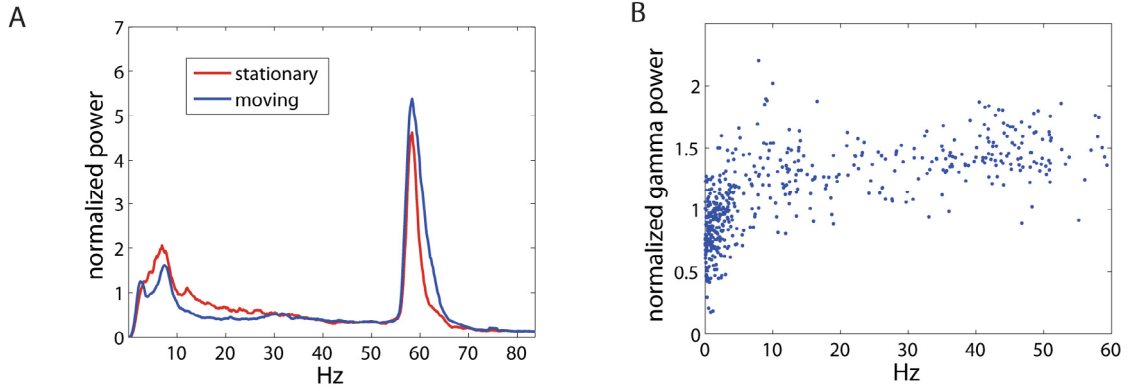
Lu, S. M., Guido, W., and Sherman, S. M. (1992). Effects of membrane voltage on receptive field properties of lateral geniculate neurons in the cat: contributions of the low-threshold Ca^{2+} conductance. *J Neurophysiol* 68, 2185-2198.

Mitra, P., and Bokil, H. (2008). *Observed brain dynamics* (Oxford ; New York, Oxford University Press).

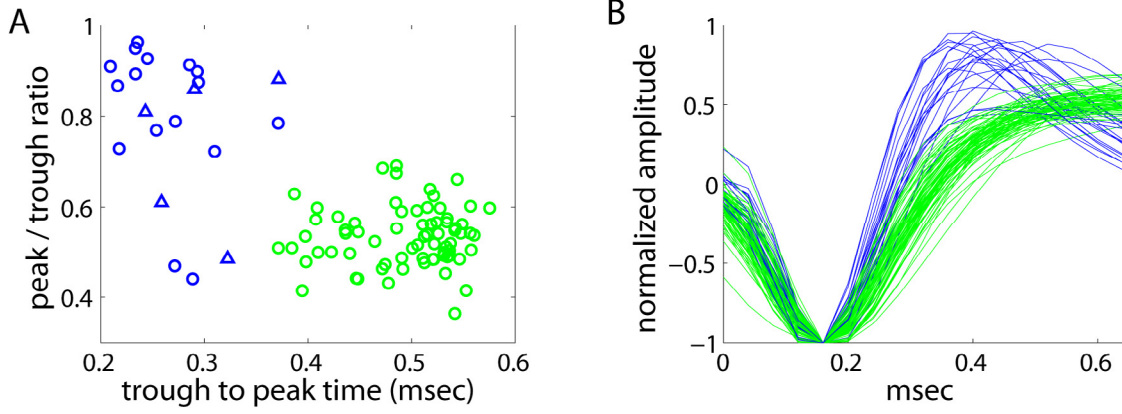
Niell, C. M., and Stryker, M. P. (2008). Highly selective receptive fields in mouse visual cortex. *J Neurosci* 28, 7520-7536.

- Pelli, D. G. (1997). The VideoToolbox software for visual psychophysics: transforming numbers into movies. *Spat Vis* *10*, 437-442.
- Remtulla, S., and Hallett, P. E. (1985). A schematic eye for the mouse, and comparisons with the rat. *Vision Res* *25*, 21-31.
- Schmitzer-Torbert, N., Jackson, J., Henze, D., Harris, K., and Redish, A. D. (2005). Quantitative measures of cluster quality for use in extracellular recordings. *Neuroscience* *131*, 1-11.
- Sirota, A., Montgomery, S., Fujisawa, S., Isomura, Y., Zugaro, M., and Buzsaki, G. (2008). Entrainment of neocortical neurons and gamma oscillations by the hippocampal theta rhythm. *Neuron* *60*, 683-697.

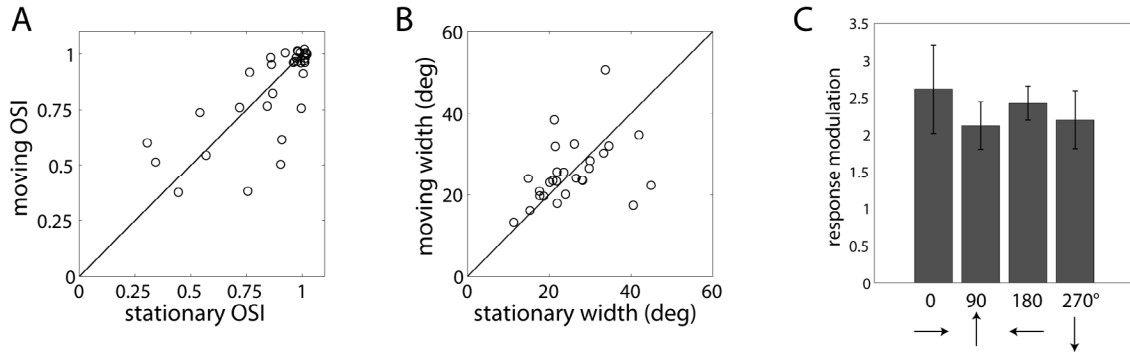
Supplemental Figure 1. The high gamma peak shows an increase with locomotion in the absence of visual stimuli on a gray mean luminance background. This peak was not present in darkness. A) Average LFP spectrum during moving versus stationary periods. B) High gamma power, from 55-65Hz, as a function of movement speed.



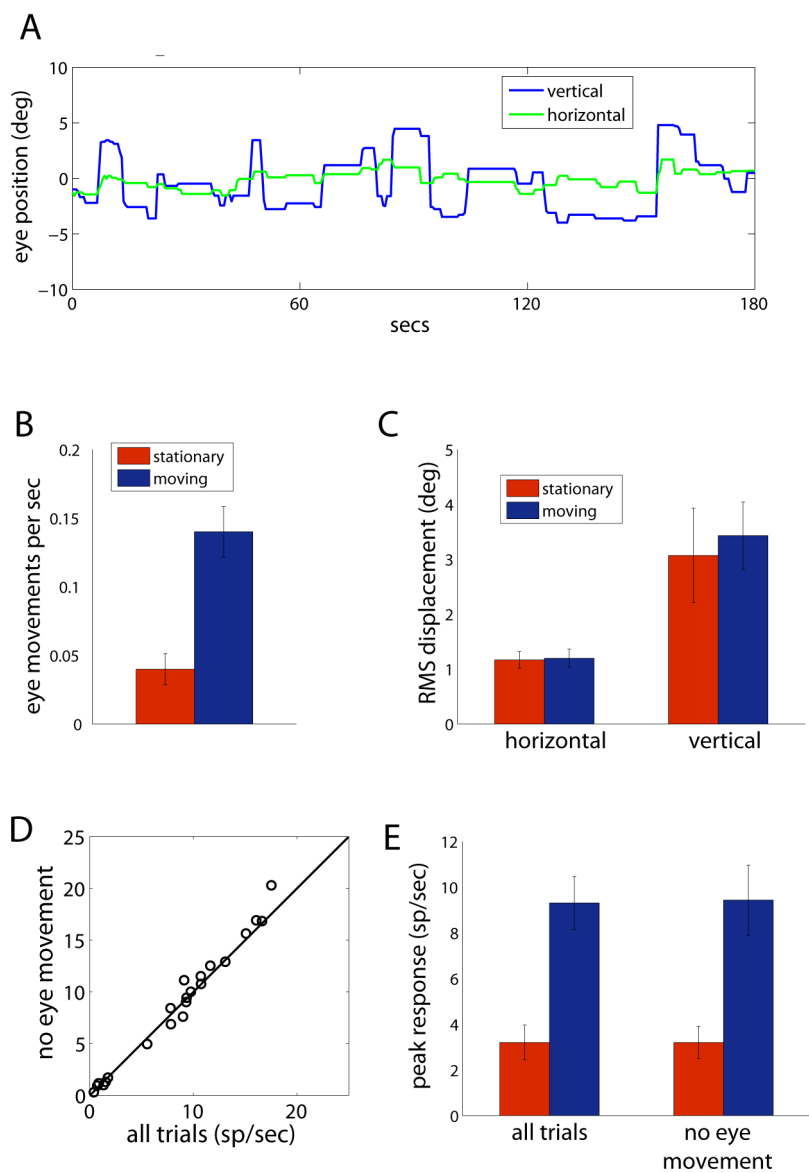
Supplemental Figure 2. Spike waveform characterization. A) Scatter plot of waveform parameters, showing narrow-spiking (blue) and broad-spiking (green). Units that showed suppressive response to stimuli are denoted by triangles. B) Average waveforms for all units, color-coded as in A.



Supplemental Figure 3. A,B) Scatter plots of orientation selectivity (A) and orientation tuning width (B), for broad-spiking units that responded in both stationary and moving states. C) Median ratio of evoked response during moving versus stationary periods, for cells preferring different directions of motion.



Supplemental Figure 4. Eye movements in awake animals. A) Example of eye movement position measured during presentation of drifting gratings. B) Mean frequency of eye movements greater than one degree. C) Root mean-square deviation of eye position. D) Peak response during movement for all trials, versus trials without eye movements, shows no significant change when eye movements are excluded. E) Median response amplitude for stationary and moving trials, with and without eye movements, demonstrating that change in response with movement is not due to the subset of trials with eye movements (n=22 units, 2 animals).



Supplemental Figure 5. Fraction of spikes that occurred in bursts in single neurons of the lateral geniculate nucleus during stationary compared to moving periods.

